ONCOIMMUNOLOGY
2016, VOL. 5, NO. 12, e1245266 (11 pages)
http://dx.doi.org/10.1080/2162402X.2016.1245266

Taylor & Francis
Taylor & Francis Group

ORIGINAL RESEARCH

OPEN ACCESS

T-cell-expressed proprotein convertase FURIN inhibits DMBA/TPA-induced skin cancer development

Maria Vähätupa[a,*], Saara Aittomäki[b,*], Zuzet Martinez Cordova[b,*], Ulrike May[a], Stuart Prince[a], Hannele Uusitalo-Järvinen[c], Tero A. Järvinen [a,d,#], and Marko Pesu[b,e,#]

[a]School of Medicine, Department of Anatomy and Cell Biology, University of Tampere, Tampere, Finland; [b]Immunoregulation, BioMediTech, University of Tampere, Tampere, Finland; [c]Department of Ophthalmology, Tampere University Hospital, Tampere, Finland; [d]Department of Orthopedics & Traumatology, Tampere University Hospital, Tampere, Finland; [e]Department of Dermatology, Tampere University Hospital, Tampere, Finland

ABSTRACT

Proprotein convertases (PCSK) have a critical role in the body homeostasis as enzymes responsible for processing precursor proteins into their mature forms. FURIN, the first characterized member of the mammalian PCSK family, is overexpressed in multiple malignancies and the inhibition of its activity has been considered potential cancer treatment. FURIN has also an important function in the adaptive immunity, since its deficiency in T cells causes an impaired peripheral immune tolerance and accelerates immune responses. We addressed whether deleting FURIN from the immune cells would strengthen anticancer responses by subjecting mouse strains lacking FURIN from either T cells or macrophages and granulocytes to the DMBA/TPA two-stage skin carcinogenesis protocol. Unexpectedly, deficiency of FURIN in T cells resulted in enhanced and accelerated development of tumors, whereas FURIN deletion in macrophages and granulocytes had no effect. The epidermises of T-cell-specific FURIN deficient mice were significantly thicker with more proliferating Ki67+ cells. In contrast, there were no differences in the numbers of the T cells. The flow cytometric analyses of T-cell populations in skin draining lymph nodes showed that FURIN T-cell KO mice have an inherent upregulation of early activation marker CD69 as well as more $CD4^+CD25^+Foxp3^+$ positive T regulatory cells. In the early phase of tumor promotion, T cells from the T-cell-specific FURIN knockout animals produced more interferon gamma, whereas at later stage the production of Th2- and Th17-type cytokines was more prominent than in wild-type controls. In conclusion, while PCSK inhibitors are promising therapeutics in cancer treatment, our results show that inhibiting FURIN specifically in T cells may promote squamous skin cancer development.

Abbreviations: CTL, cytotoxic T lymphocyte; dLN, draining lymph node; DMBA, 7,12-Dimethylbenz[a]anthracene; IFNγ, interferon gamma; IL, interleukin; KO, knockout; LysM, lysozyme-M; OVA, ovalbumin; PCSK, proprotein convertase; TCR, T-cell receptor; TGF-β1, transforming growth factor-β1; TPA, 12-O-tetradecanoylphorbol-13-acetate; Treg, regulatory T cell; VEGF, vascular endothelial growth factor

ARTICLE HISTORY
Received 25 July 2016
Revised 22 September 2016
Accepted 3 October 2016

KEYWORDS
FURIN; proprotein convertase; squamous skin cancer; T cells; transforming growth factor-β1

Introduction

The mammalian proprotein convertase (PCSK) family consists of nine members. The primarily identified seven PCSKs (PCSK1-2, FURIN, PCSK4-7) are closely related and evolutionarily conserved subtilisin/kexin-like serine proteases that convert their immature substrates into functional end-products by cleaving basic amino acid motifs ((K/R)-(X)n-(K/R)↓, where n is 0, 2, 4, or 6 and X is any amino acid).[1] PCSKs operate mainly in the secretory pathway, on the cell surface and in the endosomes. More recently identified and distantly related PCSK family members MBTPS1 and PCSK9 differ from the seven other members in their target sequence specificities. MBTPS1 targets a consensus motif (R/K)-X-(hydrophobic)-X↓ and PCSK9 has only autocatalytic cleavage activity.[2]

PCSK enzymes play an instrumental role in maintaining homeostasis in the body but also in a number of pathological conditions.[2] Various PCSK target proteins are involved in malignant transformation and progression. PCSKs activate for example cell surface-expressed receptors (e.g., integrins), tissue-modifying enzymes like matrix metalloproteinases[3-5] and growth factors needed to support tumor angiogenesis, including vascular endothelial growth factors (VEGF) C and D.[6,7] Many human cancers show high levels of PCSK expression (reviewed in ref.[8]). For example, FURIN expression is elevated in non-small cell lung

CONTACT Marko Pesu marko.pesu@uta.fi Immunoregulation, BioMediTech, University of Tampere, Lääkärinkatu 1, FI-33520 Tampere, Finland; Tero A. Järvinen tero.ah.jarvinen@uta.fi School of Medicine, Department of Anatomy and Cell Biology, University of Tampere, Lääkärinkatu 1, FI-33520 Tampere, Finland.

Supplemental data for this article can be accessed on the publisher's website.

*These authors contributed equally.

#Equal contribution and corresponding authors.

carcinoma as well as in human head and neck squamous cell carcinomas, and the upregulated FURIN activity correlates with accelerated tumor progression.[9-11] Transgenic overexpression of FURIN in mouse epidermal basal layer resulted in increased papilloma and squamous cell carcinoma development and enhanced tumor growth when the mice were subjected to a two-stage chemical carcinogenesis protocol[12]. In line with that data, deleting FURIN from mouse salivary gland cells also delayed PLAG1-induced salivary gland tumorigenesis.[13]

PCSK enzymes are also key regulators of the immune system. By using a conditional, T-cell-specific FURIN deficient mouse (CD4cre-fur$^{flox/flox}$) we have shown that T-cell-expressed FURIN is critical for maintaining peripheral tolerance.[14] T-cell-specific FURIN deletion causes age-related autoimmunity, with expansion and overactivation of effector T cells, excessive production of pro-inflammatory cytokines, and functionally defective regulatory T cells (Treg). The autoimmune phenotype in FURIN T-cell KO mice could be at least partially attributed to reduced levels of bioactive, anti-inflammatory cytokine transforming growth factor-β1 (TGF-β1), which is a known FURIN substrate molecule.[15] Furthermore, we have recently demonstrated that FURIN directly regulates T-cell activation by modifying the TCR-induced transactivation steps.[16]

The implication of PCSKs as regulators of tumor progression and metastasis has provoked an interest to use them as targets of novel anticancer agents. Based on our previous findings, inhibition of FURIN activity in immune cells could be an effective way of boosting antitumor host responses. Thus, we investigated how the immune-cell-expressed FURIN regulates tumorigenesis by using mouse strains with a conditional deletion of FURIN either in T cells or in myeloid cells (CD4cre and LysMcre, respectively) in the two-stage chemical DMBA/TPA-induced skin carcinoma model. Our data demonstrate that FURIN expression in T cells, but not in myeloid cells, constrains the DMBA/TPA-induced development of squamous skin cancer.

Results

T-cell-expressed FURIN inhibits skin tumor induction

Targeting PCSK, and in particular, FURIN activity, has been considered a promising cancer treatment.[17] However, the germ-line deletion of FURIN causes embryonic lethality, which confounds the studies on its *in vivo* functions in cancer research.[18] Therefore, the cell-type-specific function of FURIN in carcinogenesis has remained incompletely understood. To investigate if the immune-cell-expressed FURIN controls skin tumor formation, we treated the back skin of adult mice deficient for FURIN gene expression either in macrophages and granulocytes (designated LysMcre KO[19,40]) or in CD4$^+$ and CD8$^+$ T cells (designated CD4cre KO,[14]) and their respective wild-type littermates (LysM WT and CD4$^+$ WT) once with a local application of the mutagen DMBA, and then with the growth-promoting agent TPA, twice weekly for a period of 16 and 21 weeks. This treatment induces papillomas derived from the interfollicular epidermis.[20]

FURIN protein expression was detected in untreated and DMBA/TPA-treated skin in CD4$^+$ WT mice (Fig. S1). In normal skin, FURIN was expressed abundantly in the epidermis and some resident cells in the dermis were also positive for FURIN expression. DMBA/TPA application induced FURIN mRNA expression and resulted in a strong accumulation of FURIN expressing cells in the dermal part of the skin (Fig. S1).

Unexpectedly, deletion of FURIN specifically from T cells resulted in the development of more papillomas ($p < 0.0001$, Fig. 1A). The first papillomas were observed in the CD4cre KO mice 8 weeks after the beginning of the DMBA/TPA treatment, and after 9 weeks, all of the CD4cre KO mice had developed papillomas on their back skin. The first papillomas were identified in both WT control strains as well as in the LysMcre FURIN KO mice after 10–12 weeks of treatment (Fig. 1A). Furthermore, the CD4cre KO mice also developed significantly more tumors on their back skin than the other strains ($p < 0.001$, Fig. 1B). Prior to euthanization (at 17 weeks due to ethical reasons), the CD4cre KO mice had developed almost 20 papillomas per animal, whereas the WT controls had less than five papillomas on average (Fig. 1B). In addition, both LysMcre KO and LysM WT mice had a similar number of tumors at 17 weeks as CD4$^+$ WT mice. The treatment of LysMcre KO and WT strains was continued for additional 5 weeks, but no differences in tumor formation could be detected (Fig. 1B). The tumors were incident in CD4cre KO animals at a rate on average 4.6-fold greater than in CD4$^+$ WT mice during the course of experiments (negative binominal regression analysis:incidence rate ratio (IRR) = 4.6; 95% confidence interval (CI) 1.97, 10.79).

Despite CD4cre KO mice were developing skin tumors significantly faster and in greater numbers than the other strains, the papillomas in the CD4cre KO mice did not continue to grow in size (Fig. S2A). Instead, a large number of small papillomas visibly disappeared and some converted into chronic ulcers (Fig. S2B). We could not detect similar ulcers in CD4$^+$ WT, LysMcre KO, and LysM WT strains (Fig. 1C and Fig. S2). The histological analysis revealed that the ulcers in CD4cre KO mice had papilloma formations, but also ruptured epidermis and clusters of neutrophils as a sign of compromised physical integrity of the skin (Fig. S2F). In conclusion, the lack of FURIN in T cells, but not in LysM$^+$ myeloid cells, promotes tumor induction and formation in the DMBA/TPA-induced skin cancer. This prompted us to further characterize the role of T-cell-expressed FURIN in squamous skin cancer immunosurveillance.

The susceptibility to tumor formation in CD4cre FURIN KO mice is associated with enhanced cell proliferation, but not with vascularization

To understand the mechanism of the skin tumor-inhibiting function of T-cell-expressed FURIN, we first performed histological analyses to determine the epidermal and dermal thicknesses, cell proliferation (Ki67) and apoptosis (TUNEL) frequency in the back skin of DMBA/TPA treated and untreated mice.

In untreated mice, loss of FURIN from T cells resulted in a significant thickening of the epidermis (Fig. S3A). Treatment with DMBA/TPA induced a substantial increase ($p < 0.001$) in the epidermal thickness in both genotypes (both epidermises $p < 0.0001$ over untreated skin), and approximately a 30% increase in the thickness of the epidermis persisted in the CD4cre KO mice over the CD4$^+$ WT mice ($p < 0.0001$, Fig. S3A). In contrast, significant

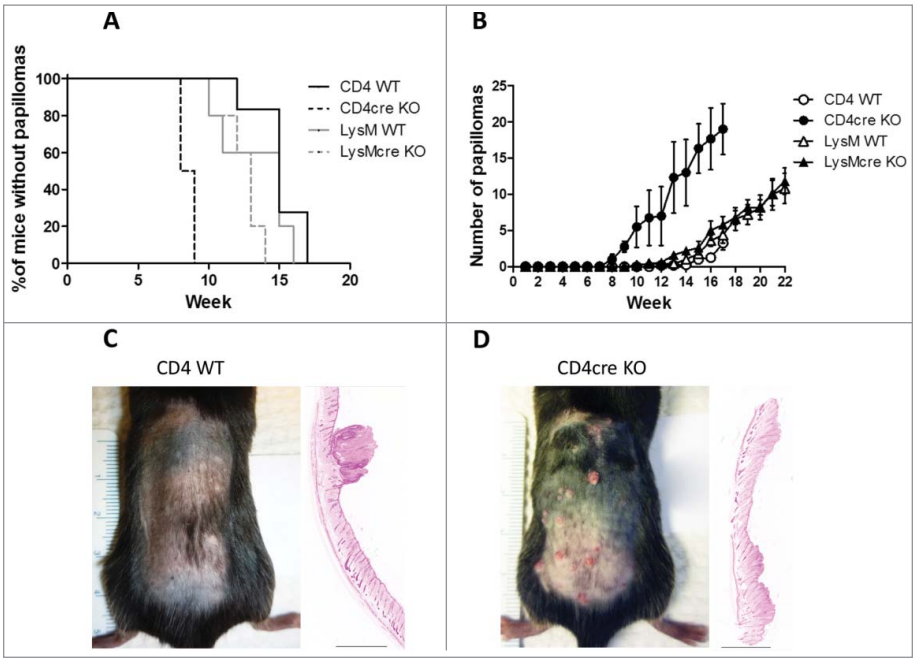

Figure 1. T-cell-specific deletion of FURIN accelerates skin tumor formation. Wild-type (LysM WT and $CD4^+$ WT), T-cell (CD4cre) and macrophage and neutrophil-specific (LysMcre) knockout mice were subjected to DMBA/TPA-induced skin carcinogenesis. (A) The percentage of tumor-free animals at each time point is shown. Survival plot was generated and analyzed via log-rank (Mantel-Cox) test. (B) The mean number of tumors per mouse at each time point is shown ± standard error of the mean. The data were analyzed using STATA 13.0 software. A non-linear regression model was used to compare the slopes of the data. (C) Representative photograph of a $CD4^+$ WT mouse at week 13 of the DMBA/TPA treatment trial, alongside a hematoxylin-eosin stained section of skin at week 17 (the black bar represents 2 mm). (D) Representative photograph of a CD4cre KO mouse at week 13 of the DMBA/TPA treatment trial, alongside a hematoxylin-eosin stained section of skin at week 17 (the black bar represents 2 mm). $CD4^+$ WT n = 6, CD4cre KO n = 4, LysM WT n=5, and LysMcre KO n = 5.

differences were not detected in the dermal thicknesses of untreated or treated animals (Fig. S3B).

CD4cre KO mice had also significantly more proliferating cells (as determined by Ki67-positivity) than WT mice in the epidermis of the untreated skin ($p < 0.0001$, Fig. S3C). After 17 weeks of DMBA/TPA treatment, the CD4cre KO mice had more proliferating cells in both epidermal and dermal parts of the skin ($p < 0.001$ and $p = 0.0056$, Figs. S3C and D). In contrast, there was no difference in the cell proliferation rate in the papilloma tissue (or the dermis beneath it) (Figs. S3C and D). TUNEL staining demonstrated that CD4cre KO mice had less apoptotic cells in untreated dermis ($p < 0.05$, Fig. S4A), but a prolonged DMBA/TPA-treatment (17 weeks) reduced significantly the numbers of dying cells in both genotypes (epidermis, $p < 0.0001$, dermis $p < 0.0001$, Fig. S4).

As the availability of vascular supply is a limiting factor for tumor growth and FURIN has a substantial influence on angiogenesis,[6,7] we also examined the vasculature in the skin. Angiogenesis is turned on already in the earliest stages of papilloma formation and in late stages the blood vessels start to increase in size.[21] There were slightly more blood vessels in CD4cre KO mice in the untreated skin compared to WT as determined by an immunohistological analysis of endothelial cell marker CD31 (Fig. S5A). A 17-week treatment with DMBA/TPA induced a 2-fold increase in the vascular density of the skin only in $CD4^+$ WT mice ($p < 0.0001$), whereas in CD4cre KO the vascular density was significantly smaller ($p < 0.0001$, Fig. S5A). Despite the fact that non-tumorous WT skin had significantly more blood vessels than in the CD4cre KO mice after the DMBA/TPA treatment, the tumor formation required vascular supply in both genotypes as evidenced by the increased number of blood vessels beneath the tumors ($p < 0.0001$, Fig. S5). In conclusion, the accelerated tumorigenesis in CD4cre KO mice was not found to be associated with increased angiogenesis.

Mice lacking FURIN in T cells have an attenuated macrophage extravasation or differentiation response to DMBA/TPA treatment

Previous work has shown that tumorigenesis in the DMBA/TPA model is promoted upon the induction of acute inflammation in the skin at the sites of chemical application.[22,23] To investigate if the CD4cre KO mice had an enhanced skin inflammatory response, we first quantified skin $CD3^+$ T cells as well as the numbers of infiltrating F4/80+ macrophages and elastase positive neutrophils. There were significantly more $CD3^+$ T cells in the CD4cre KO mice than in littermate controls in both untreated skin ($p < 0.0001$) and at 43 h post DMBA/TPA treatment ($p < 0.05$), but after 17 weeks T cell numbers were similar (Figs. 2A and B). In contrast, the numbers of macrophages were more readily induced in KO mice at 43-h time-point, but interestingly this was reverted at later stages; after a 17-week treatment CD4cre KO mice showed significantly reduced macrophage counts in non-tumorous skin ($p < 0.001$, Figs. 2C and D). The significantly lower number of macrophages in the CD4cre KO skin was especially evident underneath the papillomas, where the KO mice had only ca. twenty-five percent of the macrophages seen in the WT dermis (Figs. 2C and D). No significant differences were

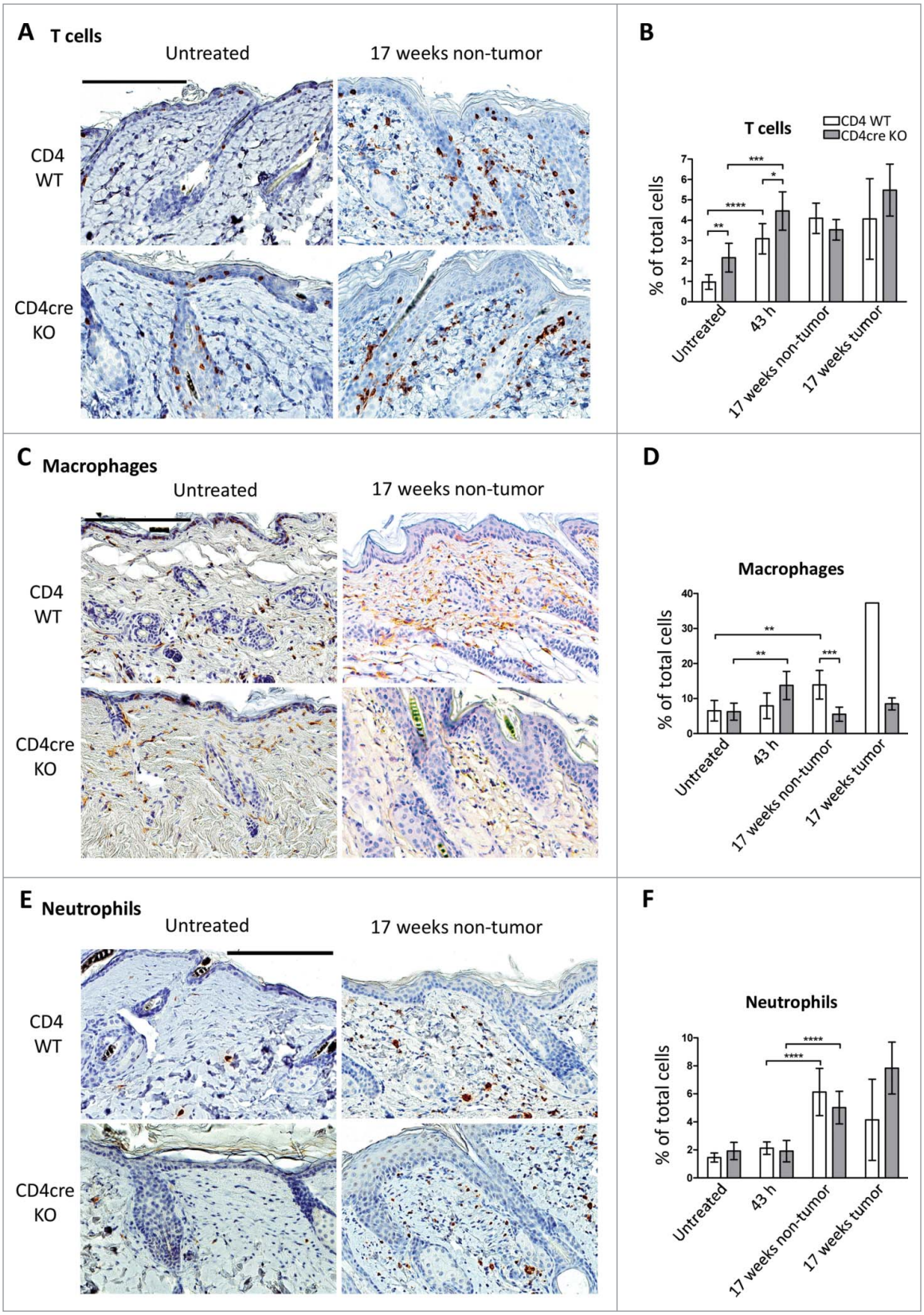

Figure 2. Immune cell numbers in the skin of WT and CD4cre FURIN KO mice. $CD4^+$ WT and CD4cre KO mice were subjected to DMBA/TPA-induced skin carcinogenesis as described in methods. Skin samples were collected from untreated animals and from mice sacrificed at 43 h after the second TPA application, and after 17 weeks of treatment (twice weekly). The skin samples were processed for IHC as described in methods. Skin sections were IHC stained for markers for T cells (CD3), macrophages (F4/80), and neutrophils (neutrophil elastase). Results are shown as mean ± 95% confidence intervals. Data were analyzed by normality tests and unpaired two-tailed Student's *t*-tests (GraphPad Prism 6). The black bar in images represents 200 μm. Nuclei are stained blue, and immune cells brown. (A) Representative photographs of T cell staining in $CD4^+$ WT and CD4cre KO skin. (B) Quantitative analyses of scanned slides were performed as described in supplementary methods. Data is expressed as % of total nuclei. (C) Representative photographs of macrophage staining and (D) results of quantitative analyses of scanned slides. (E) Representative photographs of neutrophil staining and (F) results of quantitative analyses of scanned slides. The information of animal numbers and analyzed tissue regions is shown in Table S1. ($^{****}p < 0.0001$; $^{***}p < 0.001$; $^{**}p < 0.01$; $^{*}p < 0.05$).

observed in neutrophils between the genotypes (Figs. 2E and F). Collectively these findings suggest that CD4cre KO mice may have accelerated skin immune responses at the early stage of cancer development, but this is later followed by reduced macrophage presence in cancerous skin.

The skin-draining lymph node T cells lacking FURIN display an activated phenotype

To gain specific information on the T-lymphocyte populations, the skin draining lymph node (dLN) cells from CD4cre KO mice and their WT littermate controls were subjected to flow cytometric analysis. There were no significant differences in the total $CD4^+$ T cell percentages (of total live cells) between the untreated CD4cre KO and WT mice or between CD4cre KO and WT mice treated with DMBA/TPA for 17 weeks (Fig. 3). In untreated CD4cre KO mice, there were fewer dLN $CD8^+$ T cells (percent of the live cells) than in the untreated WT controls, but the difference was lost after the 17-week DMBA/TPA treatment. However, the dLN T cells from the CD4cre KO animals displayed a more active phenotype, as significantly higher proportion of both $CD4^+$ and $CD8^+$ T cells from KO animals was positive for CD69, a marker for recently activated cells (Fig. 3).

The analysis of T-cell memory phenotypes using CD44 and CD62L antibodies demonstrated a significantly higher percentage of central memory $CD62L^{high}CD44^{high}$ $CD8^+$ T cells (of total $CD8^+$ T cells) in both untreated and 17-week-treated CD4cre KO animals (Fig. 3). This is in parallel with a recent report showing that blocking endogenous TGF-β1 signaling in $CD8^+$ T cells enhances their conversion into central memory cells.[24] Since FURIN processes pro-TGF-β1, the autocrine TGF-β1 signaling is likely to be defective in FURIN-deficient $CD8^+$ T cells. There were also significantly more $CD4^+CD25^+Foxp3^+$ Treg cells in the skin dLNs of CD4cre KO mice compared to those of WT littermates, both from untreated mice and mice treated with DMBA/TPA for 17 weeks (Fig. 3).

In conclusion, FURIN expression did not affect the numbers of T cells in the skin dLN after a 17-week DMBA/TPA-treatment, but T cells from the dLNs of the $CD4^+$ KO mice were inherently more active and constituted more of cells with a Treg phenotype, irrespective of the treatment. Therefore, the increased susceptibility of CD4cre KO mice to develop papillomas is not due to reduced dLN T-cell numbers or lack of T-cell activation.

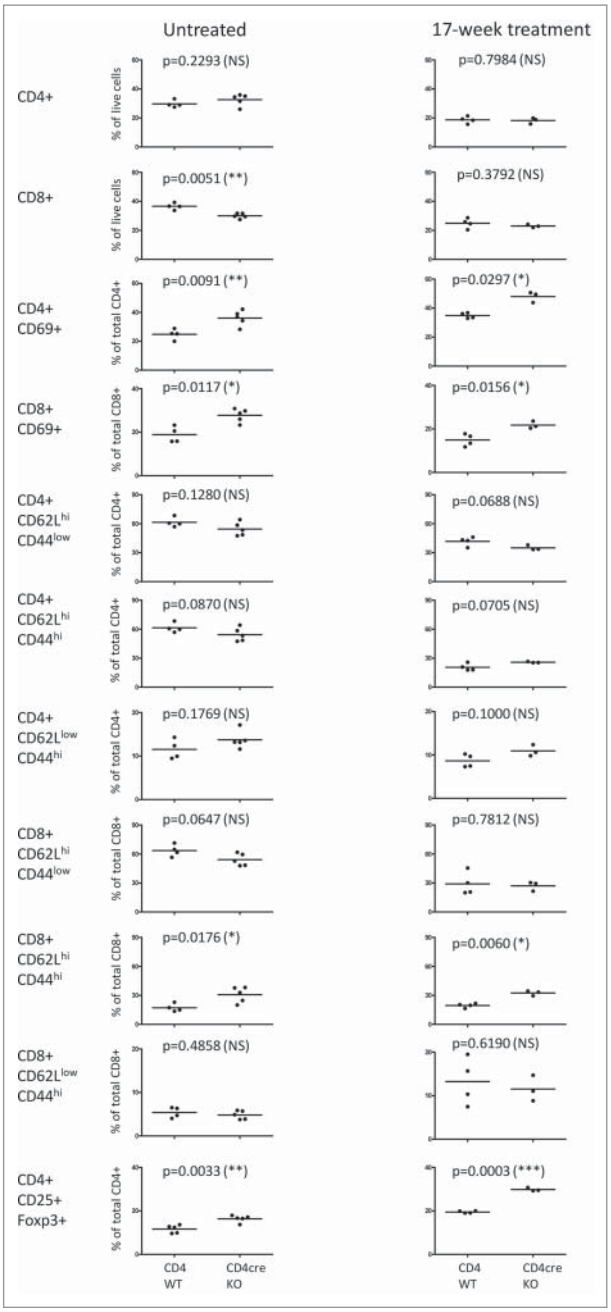

Figure 3. Profiling of the skin draining lymph node T-cell populations in WT and CD4cre KO mice. Cells were isolated from untreated mice and from animals treated with a single application of DMBA and twice-weekly doses of TPA for 17 weeks, and surface markers were analyzed by flow cytometry. Frequency of cells among total live cells or either $CD4^+$ or $CD8^+$ cell populations is shown, each symbol representing an individual mouse, lines indicating the mean. Statistics were calculated with unpaired two-tailed Student's *t*-test (with Welch correction). Untreated mice: n = 5 (for both genotypes), 17-week-treated CD4cre KO animals: n = 3, WT littermate controls n = 4.

T cells lacking FURIN produce more interferon gamma in the early phase of tumor development

To investigate the cytokine production of T cells in the early phase of tumor development, we analyzed dLN T cells at 48 h post the second TPA treatment by intracellular staining and flow cytometry. Both $CD4^+$ and $CD8^+$ effector T cells from the CD4cre KO mice produced more pro-inflammatory interferon gamma (IFNγ) (Figs. 4B and C). On the other hand, there was no difference in the production of another pro-inflammatory cytokine, interleukin (IL) 17A (IL-17A), or in the $CD4^+$ T-cell-produced IL-10, which is considered anti-inflammatory (Figs. 4B and C). In order to gain information on the predominant type of immune response in the CD4cre KO mice and their WT controls, we analyzed the systemic production of various chemokines, by performing a multiplex assay from the sera 43 h post second TPA treatment. There were no obvious differences in the levels of CCL2/MCP1, CXCL-1/GROα, CCL11/Eotaxin, CXCL2/MIP-2, CCL7/MCP-3, CCL5/RANTES, CCL3/MIP-1α, or CCL4/MIP-1β (data not shown), but the level of CXCL10/IP-10 was elevated by 2-folds in CD4cre KO sera compared to those of WT mice ($p = 0.0711$, Fig. 4E). Collectively, these findings imply that in the early

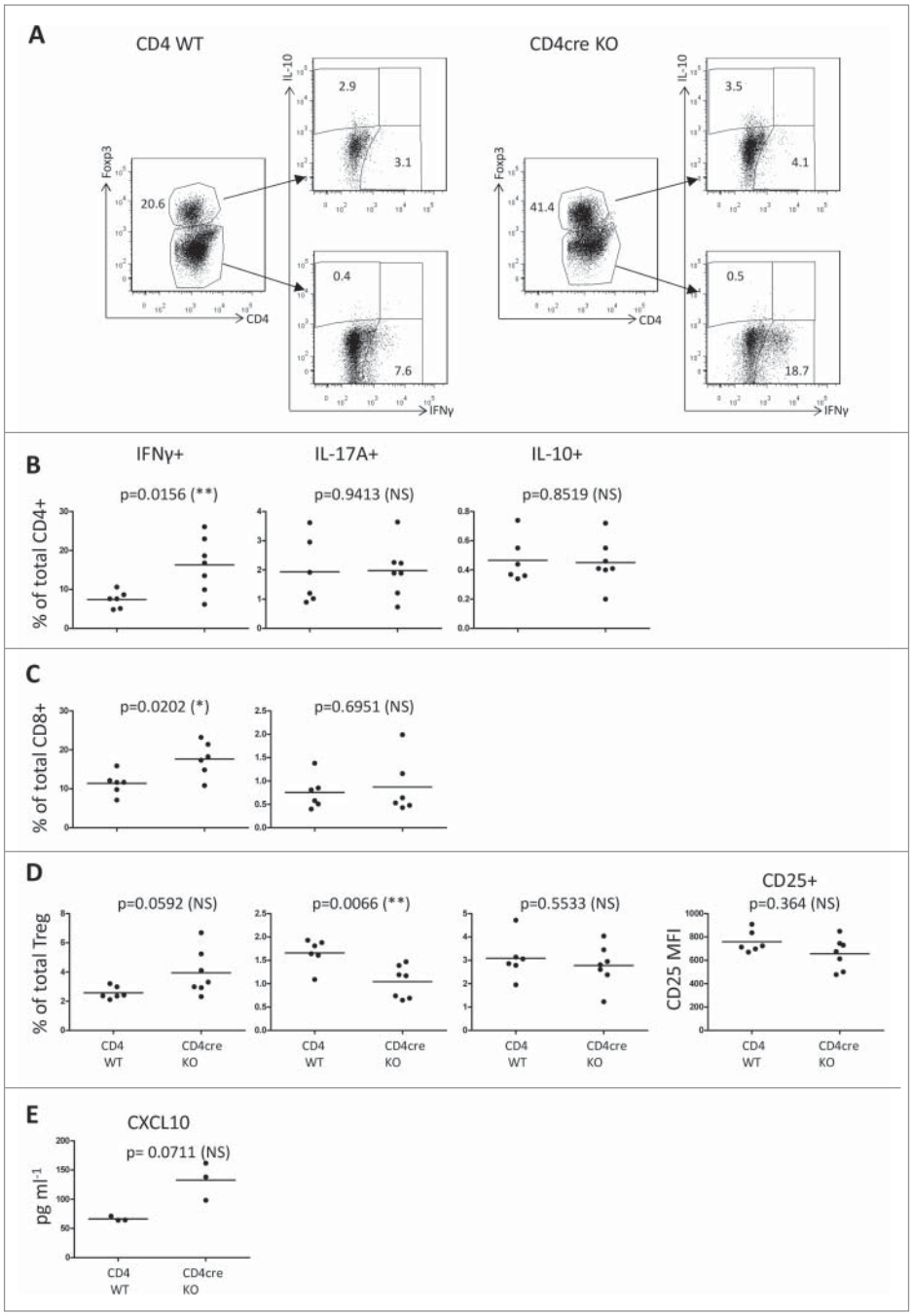

Figure 4. T cells from the skin draining lymph nodes of CD4cre KO mice show elevated IFNγ production in the early phase of tumor development. Intracellular flow cytometry from skin draining lymph node cells. Mice were treated with one dose of DMBA, two doses of TPA on the back skin, then sacrificed after 48 h from the 2nd TPA dose, and the isolated dLN cells were stimulated with TPA + Ca-ionomycin for 4 h *in vitro*. (A) Representative plots from $CD4^+$ WT and CD4cre KO mice, showing live-gated cell populations positive for $CD4^+$, Foxp3, IFNγ, and IL-10. (B) Percentages of $CD4^+$ cells positive for IFNγ, IL-17A, and IL-10. (C) $CD8^+$ cells positive for IFNγ and IL-17A. (D) $CD4^+Foxp3^+$ Treg positive for IFNγ, IL-17A, and IL-10, and the mean fluorescence intensity (MFI) of CD25 from the Treg population. (E) CXCL10 levels from sera from mice treated with TPA for 43 h, determined by the ProCartaPlex Mouse Cytokine & Chemokine 26-plex assay and Bio-Plex 200 instrument. B, C, D: $CD4^+$ WT mice n = 6, CD4cre KO mice n = 7; E: $CD4^+$ WT mice n = 3, CD4cre KO mice n = 3. Each symbol represents an individual mouse, lines indicate the mean. Statistics: Unpaired two-tailed Student's *t*-test with Welch correction.

phase of tumor development the FURIN T-cell-specific knockout mice have a Th1-type-skewed immune response.[25]

We also studied the production of IFNγ, IL-17A, and IL-10 by $CD4^+Foxp3^+$ Treg cells isolated from the dLNs of CD4cre KO and WT mice. There was a trend toward a higher production of IFNγ in the Treg cells from the CD4cre KO animals ($p = 0.0592$), and a significant reduction in the percentage of CD4cre KO Treg cells positive for IL-17A ($p = 0.0066$, Fig. 4D). However, the percentage of dLN Treg cells producing IL-10 was not different between the CD4cre KO and WT. Also the mean fluorescence intensity of the CD25 surface staining was similar in Treg cells isolated from dLNs of both CD4cre KO and WT mice indicating normal Treg activation status.

Collectively, the flow cytometric analyses suggest that the tendency of CD4cre KO animals to develop more papillomas could be related to accelerated Th1-type immune responses.[26] In contrast, despite CD4cre KO animals showing an increased number of regulatory $CD4^+CD25^+Foxp3^+$ cells, these cells are

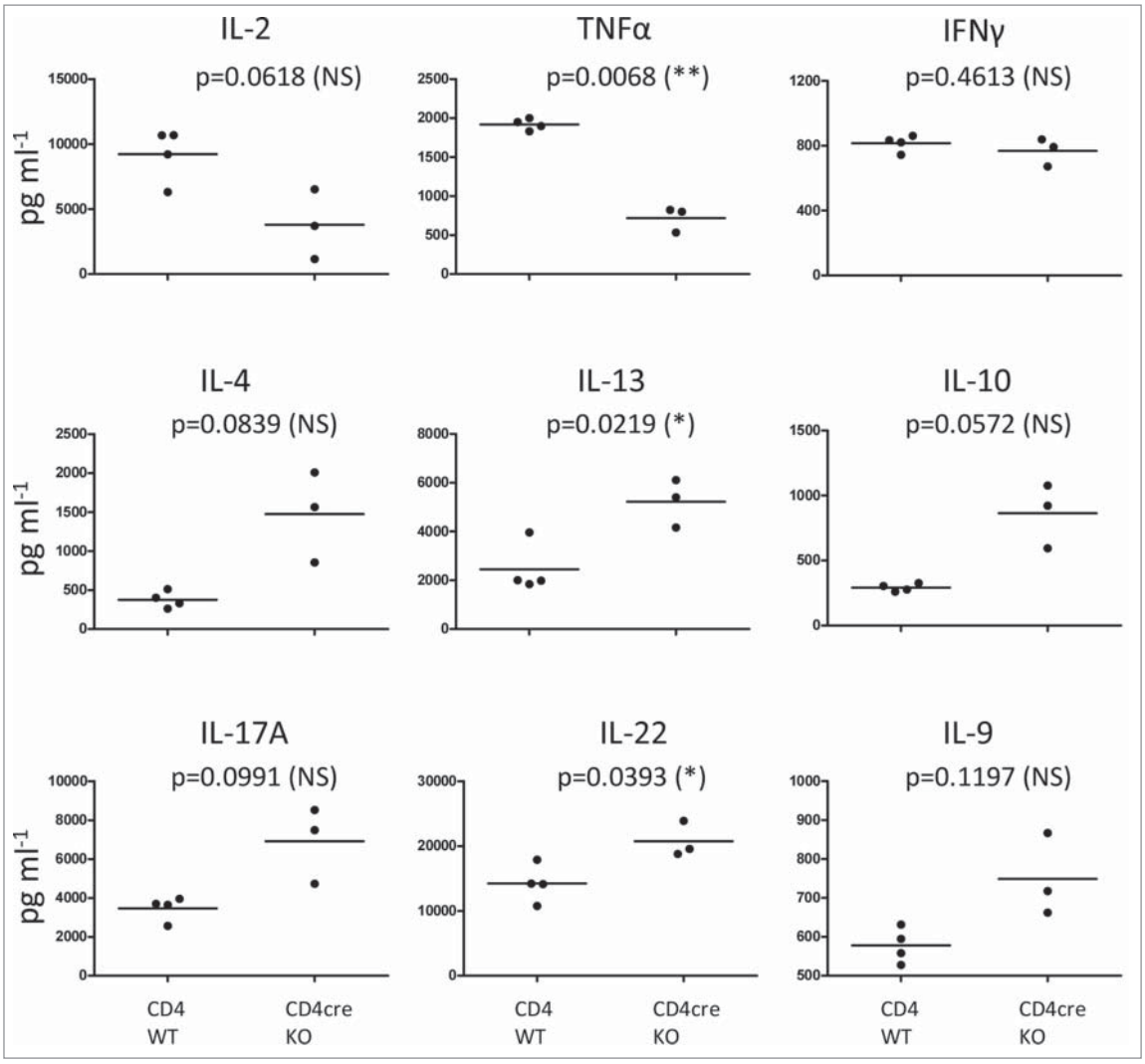

Figure 5. FURIN-deficient T cells show a Th2- and Th17-type cytokine profile of in the late phase of tumor progression. CD4cre KO and WT mice were treated once with DMBA, then with TPA for 17 weeks (twice a week) on the back skin as in Fig. 1. At 17 weeks, animals were sacrificed and skin draining lymph node cells were cultured for 48 h in the presence of plate-bound anti-CD3 and soluble anti-CD28 antibodies. Cytokine levels were determined from the culture supernatants with ProCartaPlex Mouse Cytokine & Chemokine 26-plex assay and Bio-Plex 200 instrument, or for IFNγ, with ELISA. Statistics: Unpaired two-tailed Student's *t*-test with Welch correction. $CD4^+$ WT n = 4, CD4cre KO n = 3. Each symbol represents an individual mouse, lines indicate the mean.

likely defective in their suppressive activity as suggested by upregulated CD69 expression and IFNγ production in $CD4^+$, $CD8^+$ effector T cells, and Tregs. This conclusion is also supported by our previous data demonstrating impaired peripheral Treg-dependent immune tolerance in CD4cre KO mice.[14]

In the later stage of carcinogenesis T-cell responses in the FURIN deficient T cells switch toward Th2 and Th17 type

In addition to T-cell activation, FURIN regulates the T helper cell balance of the immune system.[27,28] We profiled the levels of multiple cytokines and chemokines from the cells isolated from skin dLNs of the mice that had been treated with DMBA/TPA for 17 weeks. Surprisingly, the cells from CD4cre KO mice no longer produced elevated IFNγ levels (like in the early phase), but the production of Th2-type cytokine IL-13 and Th17-type cytokine IL-22 was higher ($p = 0.0219$ and $p = 0.0393$, respectively, Fig. 5). Also, the levels of other Th2/Th17 cytokines, IL-4, IL-17A, IL-9, or IL-10 showed a trend toward upregulated production in the CD4cre KO animals (Fig. 5). QRT-PCR performed from the back skins confirmed the switch in Th responses, showing an upregulation of *IFNγ* in the KO animals in the early time points and of *IL-17a* in the late time point (Fig. S6). The levels of IL-2 and tumor necrosis factor α (TNFα) were lower in the dLN cells isolated from CD4cre KO mice compared to those isolated from WT animals, as we have previously shown in the untreated animals.[14] Altogether, the results suggest that during the course of carcinogenesis progression, the early Th1-biased immune responses of the T-cell-specific FURIN deficient mice switch increasingly toward Th2 and Th17 type responses. Thus, FURIN has an inherent role in modulating T helper cell balance in a chronic immune insult.

Discussion

Various studies have shown that FURIN overexpression is associated with accelerated carcinogenesis. Thus, its inhibition could be a viable cancer treatment. However, the function of

FURIN in different cell types that contribute to tumor formation is poorly characterized. To study the role of FURIN in immune cells in the context of squamous skin cancer development, we utilized two mouse strains that lack FURIN specifically either in macrophages and granulocytes or in T cells.

As our previous results have shown that FURIN-deficient T cells and macrophages display an overtly activated phenotype,[14,19,40] we assumed that the FURIN-deficient immune cells might be more effective in anticancer immune responses. However, after being subjected to the DMBA/TPA treatment, mice with the T-cell-specific knockdown of FURIN (CD4cre KO) developed more papillomas and they appeared faster in the knockout than their WT littermates. The CD4cre KO mice presented with a thicker epidermis, with more epidermal cell proliferation than the WT mice, and this difference between the genotypes was maintained after 17 weeks of DMBA/TPA treatment. Under normal conditions, the CD4cre KO skin harbored more $CD3^+$ T cells than the WT skin, but upon treatment that difference was lost. Analysis of skin dLN cells showed no major FURIN-dependent effects of the DMBA/TPA treatment on the numbers of $CD4^+$ or $CD8^+$ T-cell populations. The higher number of $CD4^+CD25^+Foxp3^+$ Tregs present in CD4cre KO dLNs in the steady state persisted after the treatment, as did the number of activated $CD4^+CD69^+$ and $CD8^+CD69^+$ T cells. In the early phase of tumor promotion, the CD4cre KO mice had more pro-inflammatory IFNγ-producing T cells, whereas CD4cre KO dLN cells secreted more Th2- and Th17-type cytokines after 17 weeks of DMBA/TPA treatment (Fig. S7).

The fact that CD4cre KO, but not LysMcre KO, mice had an increased susceptibility for papilloma development is in line with several studies showing a tumor-enhancing role for $\alpha\beta$ T cells.[29,30] Previous work has demonstrated that IFNγ promotes tumor development primarily in the early stage of papilloma development.[26] IL-17A, in turn, has a role in the promotion process in both human non-melanoma skin cancer and mouse models of skin cancer, suggesting that Th2- and Th17-type cytokine profile of the T cells lacking FURIN could be driving the carcinogenesis process at later stages.[31-33] LysMcre KO mice, in contrast, display accelerated innate immunity responses, and a heterozygous, inactivating mutation in the *FurinA* gene results in enhanced innate responses in *Mycobacterium marinum* –infected zebrafish.[19,40] However, the pro-inflammatory phenotype due to lack of FURIN in myeloid cells does not seem to play a major role in the papilloma development in the DMBA/TPA-model.

FURIN and other PCSK family members play an important role in carcinogenesis and metastasis, and there has been considerable interest to develop pharmaceutical inhibitors of their activity for cancer treatment. Inhibiting FURIN/PCSK is reasoned to directly block the processing of factors that are associated with tumor invasion and metastatic activity, including matrix metalloproteinases, growth factors, and others. Furthermore, FURIN is critical for the activation of anti-inflammatory cytokine TGF-β1. Thus, specific blocking of FURIN is thought to support antitumor host-responses by promoting cancer immunosurveillance. The assessment of a bifunctional GM-CSF-FURINshRNA construct (FANG^{TM}, Vigil^{TM}, Gradalis) has already entered the phase II clinical trials for treatment of melanoma, ovarian cancer, and colorectal cancer with liver metastasis.[17,34] Recently, the shRNA-mediated inhibition of FURIN together with dendritic cell supporting GM-CSF expression was also found to be efficacious in metastatic, advanced Ewing's sarcoma.[35] In contrast, in liver cancers FURIN overexpression suppresses tumor growth and predicts better postoperative survival.[36] The beneficial effect of FURIN in hepatocellular carcinoma was also reported in mice where FURIN was deleted using liver specific Albumin CRE.[37] It seems therefore plausible that FURIN has tumor type-specific effects, and thus FURIN inhibition systematically may not always be beneficial for oncology patients.

The role of FURIN in T-cell-dependent immunity is clearly multifaceted. A major function of FURIN is to control the bioavailability of anti-inflammatory TGF-β1, and Treg-dependent peripheral immune tolerance.[14] TGF-β1 is a multifunctional growth factor that has roles in both promoting and suppressing tumorigenesis.[38] Deleting TGF-β1 specifically from activated $CD4^+$ T cells and Treg cells reduced metastatic B16-OVA tumor cell spread to the mouse lung, indicating that activated $CD4^+$ T-cell-derived TGF-β1 inhibits tumor immunosurveillance.[39] Importantly, we have also shown that FURIN is an important factor in modulating the T helper cell balance. Mice that were chronically infected with intracellular *Toxoplasma gondii* parasite had less pathogen-specific Th1-type immune cells, and naïve, OVA-specific FURIN KO $CD4^+$ T cells showed an increased tendency to polarize into the IL-4-producing Th2 cells.[27] The switch from Th1 into Th2/Th17-type responses was also seen here in CD4cre KO mice after a 17-week DMBA/TPA treatment. Thus, inhibiting FURIN does not just promote T-cell-driven adaptive immunity, but it also modulates the type of T helper cell responses. It is also noteworthy that the regulatory role of FURIN in $CD8^+$ cytotoxic lymphocytes remains incompletely understood. Our data showed that FURIN-deficient CTLs produced more IFNγ and showed an upregulation of CD69 activation marker, but a careful analysis of for example their cytotoxic potential, granzyme B, and perforin expressions needs further studies.

In conclusion, our data demonstrate that FURIN expression in T cells clearly modulates adaptive immune responses in both untreated mice and in animals suffering from DMBA/TPA-induced skin papillomas. This leads to accelerated tumor development accompanied with aberrant T-cell cytokine production in T-cell-specific FURIN KO mice. Our findings suggest that inhibiting FURIN systematically, or specifically in T cells, may promote the development of cancer types wherein a chronic immune insult has a cancer provoking role. This is an important aspect when considering FURIN inhibitors' therapeutic potential in human cancers.

Materials and methods

Mice

T-cell-specific FURIN conditional knockout (CD4cre KO) mice on a C57BL/6 background have been described previously.[14,27] Macrophage-specific FURIN conditional knockout mice (LysMcre KO) were generated using a LysMcre C57BL/6 background.[19,40] Mice were fed with standard laboratory pellets and

water *ad libitum*. All animal experiments were performed in accordance with protocols approved by the National Animal Ethics Committee of Finland.

Skin tumor induction

Both FURIN KO strains, LysMcre and CD4cre, as well as their respective littermate control C57BL/6 WT, LysM WT and $CD4^+$ WT mice were treated with DMBA and TPA to induce skin tumors as previously described.[22] In brief, the backs of 8–14-week-old mice were shaved and 24 h later 50 μg DMBA (7,12-Dimethylbenz[a]anthracene) (Sigma, Dorset, UK) in 200 μL acetone was applied topically on the shaved area of the dorsal skin. After a week, the back skin of the mice was treated twice a week with 5 μg TPA (12-*O*-tetradecanoylphorbol-13-acetate) (Sigma) in 200 μL acetone for 16 or 21 weeks. The fur excluding tumors was carefully shaved every 2 weeks. Tumors (1 mm in diameter or larger) were counted twice a week and changes in tumor development were recorded for each individual tumor.

Immunohistochemical (IHC) and TUNEL staining

Samples of back skin from sacrificed, shaved control mice or mice at 43 h or week 17 of the tumor induction experiment were collected and fixed with 4% paraformaldehyde and embedded in paraffin according to standard protocols. Hematoxylin/eosin staining and DAB immunohistochemical staining (IHC) was performed on 6-μm thick paraffin sections as previously described.[22] The following primary antibodies were used for IHC: A0452 rabbit anti-CD3 (DakoCytomation, Glostrup, Denmark), MF48000 BM8 rat anti-F4/80 (Life Technologies Ltd., Paisley, UK), and 68672 rabbit anti-neutrophil elastase (AbCam, Cambridge, UK). More detailed list of reagents, imaging, and quantitation are described in the Supplementary methods.

Flow cytometry

For surface markers, the skin dLN cells were stained with antibodies against mouse CD4, CD8, CD44, CD62L, and CD69 (all from eBioscience, San Diego, California, USA). For intracellular staining, isolated dLN cells were stimulated with PMA and Caionomycin for 4 h, and Brefeldin A and Monensin were applied for the last 2 h of the stimulation. The cells were stained with surface markers and subsequently fixed overnight with Fixation/Permeabilization solution (from Foxp3/Transcription Factor Staining Buffer Set, eBioscience), permeabilized with Permeabilization Buffer (eBioscience) and stained with intracellular antibodies (IL-10, IFNγ, IL-17A, Foxp3; all from eBioscience), according to the manufacturer's instructions. All cells were analyzed with FACSCanto II (Becton, Dickinson and Company, Franklin Lakes, New Jersey, USA), data analysis performed with FlowJo software (Flowjo LLC, Ashland, Oregon, USA).

Luminex and ELISA assays

Skin dLN cells from mice treated with DMBA/TPA for 17 weeks were cultured for 48 h in the presence of plate-bound anti-CD3 antibody (10 μg/mL, clone 17A2, eBioscience) and soluble anti-CD28 Ab (2 μg/mL, clone 37.51, eBioscience). Multiplex cytokine/chemokine measurement was done from the culture supernatants using ProCartaPlex assay (Mouse Cytokine & Chemokine 26-plex, eBioscience) according to the manufacturer's instructions, and with Bio-Plex 200 instrument (Bio-Rad). IFNγ levels were determined from the cell culture supernatants with a Ready-Set-Go! ELISA kit (eBioscience), according to the manufacturer's instructions.

Statistical analysis

Mean averages are shown with 95% confidence intervals, in the case of Fig. 1B with SEM. Immunohistochemistry data were analyzed to determine if it was normally distributed (D'Agostino & Pearson omnibus and Shapiro–Wilk normality tests). Significance at a given time point was calculated by two-tailed Student's *t*-test for normally distributed data. An α level less than 0.05 was considered significant. Tumor-free survival plot data were analyzed by log-rank (Mantel-Cox) test and non-normally distributed time course data were analyzed by non-linear regression. Prism 6 (GraphPad Software, La Jolla California, USA) was used for a majority of the analyses and STATA 13.0 (StataCorp LP, College Station, Texas, USA:) statistical analysis software was used for non-linear negative binomial regression analysis, as indicated.

Disclosure of potential conflicts of interest

No potential conflicts of interest were disclosed.

Acknowledgments

We thank Marianne Karlsberg, Marja-Leena Koskinen, and Anni Laitinen for practical support and Heini Huhtala for statistical advice. Mrs. Guillermina Garcia (Sanford-Burnham-Prebys Medical Discovery Institute, La Jolla, CA, USA) is thanked for her technical expertise and help with quantitative microscopy.

Funding

The work was funded by the Sigrid Juselius Foundation, the Academy of Finland, Päivikki and Sakari Sohlberg Foundation, Instrumentarium Research Foundation, Finnish Medical Foundation, Pirkanmaa Hospital District Research Foundation, the Finnish Cultural Foundation, the University of Tampere Foundation, Biocenter Finland, Competitive Research Funding of the Tampere University Hospital, Cancer Society of Finland, and Tampere Tuberculosis Foundation.

Author contributions

T.J., M.V., M.P., S.A., H.U.-J., and Z.M.C. designed the research. M.V., S. A., Z.M.C., and U.M. performed the research. M.V., S.P., S.A., Z.M.C., and U.M. analyzed the data. T.J., M.V., U.M., S.A., and M.P. wrote the manuscript. M.V., S.A., and U.M. made the figures. M.V., S.P., U.M., S.A., H.U.-J., M.P., and T.J. reviewed and edited the paper.

ORCID

Tero A. Järvinen http://orcid.org/0000-0002-4027-1759

References

1. Turpeinen H, Ortutay Z, Pesu M. Genetics of the first seven proprotein convertase enzymes in health and disease. Curr Genomics 2013; 14:453-67; PMID:24396277; http://dx.doi.org/10.2174/1389202911314050010
2. Artenstein AW, Opal SM. Proprotein convertases in health and disease. N Engl J Med 2011; 365:2507-18; PMID:22204726; http://dx.doi.org/10.1056/NEJMra1106700
3. Sato H, Kinoshita T, Takino T, Nakayama K, Seiki M. Activation of a recombinant membrane type 1-matrix metalloproteinase (MT1-MMP) by furin and its interaction with tissue inhibitor of metalloproteinases (TIMP)-2. FEBS Lett 1996; 393:101-4; PMID:8804434; http://dx.doi.org/10.1016/0014-5793(96)00861-7
4. Remacle AG, Rozanov DV, Fugere M, Day R, Strongin AY. Furin regulates the intracellular activation and the uptake rate of cell surface-associated MT1-MMP. Oncogene 2006; 25:5648-55; PMID:16636666; http://dx.doi.org/10.1038/sj.onc.1209572
5. Koo BH, Kim HH, Park MY, Jeon OH, Kim DS. Membrane type-1 matrix metalloprotease-independent activation of pro-matrix metalloprotease-2 by proprotein convertases. FEBS J 2009; 276:6271-84; PMID:19780834; http://dx.doi.org/10.1111/j.1742-4658.2009.07335.x
6. Siegfried G, Basak A, Cromlish JA, Benjannet S, Marcinkiewicz J, Chretien M, Seidah NG, Khatib AM. The secretory proprotein convertases furin, PC5, and PC7 activate VEGF-C to induce tumorigenesis. J Clin Invest 2003; 111:1723-32; PMID:12782675; http://dx.doi.org/10.1172/JCI200317220
7. McColl BK, Paavonen K, Karnezis T, Harris NC, Davydova N, Rothacker J, Nice EC, Harder KW, Roufail S, Hibbs ML et al. Proprotein convertases promote processing of VEGF-D, a critical step for binding the angiogenic receptor VEGFR-2. FASEB J 2007; 21:1088-98; PMID:17242158; http://dx.doi.org/10.1096/fj.06-7060com
8. Bassi DE, Fu J, Lopez de Cicco R, Klein-Szanto AJ. Proprotein convertases: "master switches" in the regulation of tumor growth and progression. Mol Carcinog 2005; 44:151-61; PMID:16167351; http://dx.doi.org/10.1002/mc.20134
9. Schalken JA, Roebroek AJ, Oomen PP, Wagenaar SS, Debruyne FM, Bloemers HP, Van de Ven WJ. Fur Gene Expression as a Discriminating Marker for Small Cell and Nonsmall Cell Lung Carcinomas. J Clin Invest 1987; 80:1545-9; PMID:2824565; http://dx.doi.org/10.1172/JCI113240
10. Bassi DE, Mahloogi H, Al-Saleem L, Lopez De Cicco R, Ridge JA, Klein-Szanto AJ. Elevated furin expression in aggressive human head and neck tumors and tumor cell lines. Mol Carcinog 2001; 31:224-32; PMID:11536372; http://dx.doi.org/10.1002/mc.1057
11. Bassi DE, Lopez De Cicco R, Mahloogi H, Zucker S, Thomas G, Klein-Szanto AJ. Furin inhibition results in absent or decreased invasiveness and tumorigenicity of human cancer cells. Proc Natl Acad Sci U S A 2001; 98:10326-31; PMID:11517338; http://dx.doi.org/10.1073/pnas.191199198
12. Fu J, Bassi DE, Zhang J, Li T, Nicolas E, Klein-Szanto AJ. Transgenic overexpression of the proprotein convertase furin enhances skin tumor growth. Neoplasia 2012; 14:271-82; PMID:22577343; http://dx.doi.org/10.1593/neo.12166
13. De Vos L, Declercq J, Rosas GG, Van Damme B, Roebroek A, Vermorken F, Ceuppens J, van de Ven W, Creemers J. MMTV-cre-mediated fur inactivation concomitant with PLAG1 proto-oncogene activation delays salivary gland tumorigenesis in mice. Int J Oncol 2008; 32:1073-83; PMID:18425334; http://dx.doi.org/10.3892/ijo.32.5.1073
14. Pesu M, Watford WT, Wei L, Xu L, Fuss I, Strober W, Andersson J, Shevach EM, Quezado M, Bouladoux N et al. T-cell-expressed proprotein convertase furin is essential for maintenance of peripheral immune tolerance. Nature 2008; 455:246-50; PMID:18701887; http://dx.doi.org/10.1038/nature07210
15. Dubois CM, Blanchette F, Laprise MH, Leduc R, Grondin F, Seidah NG. Evidence that furin is an authentic transforming growth factor-beta1-converting enzyme. Am J Pathol 2001; 158:305-16; PMID:11141505; http://dx.doi.org/10.1016/S0002-9440(10)63970-3
16. Ortutay Z, Oksanen A, Aittomaki S, Ortutay C, Pesu M. Proprotein convertase FURIN regulates T cell receptor-induced transactivation. J Leukoc Biol 2015; 98:73-83; PMID:25926688; http://dx.doi.org/10.1189/jlb.2A0514-257RR
17. Senzer N, Barve M, Kuhn J, Melnyk A, Beitsch P, Lazar M, Lifshitz S, Magee M, Oh J, Mill SW et al. Phase I trial of "bi-shRNAi(furin)/GMCSF DNA/autologous tumor cell" vaccine (FANG) in advanced cancer. Mol Ther 2012; 20:679-86; PMID:22186789; http://dx.doi.org/10.1038/mt.2011.269
18. Roebroek AJ, Umans L, Pauli IG, Robertson EJ, van Leuven F, Van de Ven WJ, Constam DB. Failure of ventral closure and axial rotation in embryos lacking the proprotein convertase Furin. Development 1998; 125:4863-76; PMID:9811571
19. Ojanen MJ, Turpeinen H, Cordova ZM, Hammaren MM, Harjula SK, Parikka M, Ramet M, Pesu M. The proprotein convertase subtilisin/kexin furinA regulates zebrafish host response against Mycobacterium marinum. Infect Immun 2015; 83:1431-42; PMID:25624351; http://dx.doi.org/10.1128/IAI.03135-14
20. Perez-Losada J, Balmain A. Stem-cell hierarchy in skin cancer. Nat Rev Cancer 2003; 3:434-43; PMID:12778133; http://dx.doi.org/10.1038/nrc1095
21. Bolontrade MF, Stern MC, Binder RL, Zenklusen JC, Gimenez-Conti IB, Conti CJ. Angiogenesis is an early event in the development of chemically induced skin tumors. Carcinogenesis 1998; 19:2107-13; PMID:9886564; http://dx.doi.org/10.1093/carcin/19.12.2107
22. May U, Prince S, Vahatupa M, Laitinen AM, Nieminen K, Uusitalo-Jarvinen H, Jarvinen TA. Resistance of R-Ras knockout mice to skin tumour induction. Sci Rep 2015; 5:11663; PMID:26133397; http://dx.doi.org/10.1038/srep11663
23. Swann JB, Vesely MD, Silva A, Sharkey J, Akira S, Schreiber RD, Smyth MJ. Demonstration of inflammation-induced cancer and cancer immunoediting during primary tumorigenesis. Proc Natl Acad Sci U S A 2008; 105:652-6; PMID:18178624; http://dx.doi.org/10.1073/pnas.0708594105
24. Takai S, Schlom J, Tucker J, Tsang KY, Greiner JW. Inhibition of TGF-beta1 signaling promotes central memory T cell differentiation. J Immunol 2013; 191:2299-307; PMID:23904158; http://dx.doi.org/10.4049/jimmunol.1300472
25. Bonecchi R, Bianchi G, Bordignon PP, D'Ambrosio D, Lang R, Borsatti A, Sozzani S, Allavena P, Gray PA, Mantovani A et al. Differential expression of chemokine receptors and chemotactic responsiveness of type 1 T helper cells (Th1s) and Th2s. J Exp Med 1998; 187:129-34; PMID:9419219; http://dx.doi.org/10.1084/jem.187.1.129
26. Xiao M, Wang C, Zhang J, Li Z, Zhao X, Qin Z. IFNgamma promotes papilloma development by up-regulating Th17-associated inflammation. Cancer Res 2009; 69:2010-17; PMID:19244111; http://dx.doi.org/10.1158/0008-5472.CAN-08-3479
27. Oksanen A, Aittomaki S, Jankovic D, Ortutay Z, Pulkkinen K, Hamalainen S, Rokka A, Corthals GL, Watford WT, Junttila I et al. Proprotein convertase FURIN constrains Th2 differentiation and is critical for host resistance against Toxoplasma gondii. J Immunol 2014; 193:5470-9; PMID:25355923; http://dx.doi.org/10.4049/jimmunol.1401629
28. Pesu M, Muul L, Kanno Y, O'Shea JJ. Proprotein convertase furin is preferentially expressed in T helper 1 cells and regulates interferon gamma. Blood 2006; 108:983-5; PMID:16627761; http://dx.doi.org/10.1182/blood-2005-09-3824
29. Girardi M, Glusac E, Filler RB, Roberts SJ, Propperova I, Lewis J, Tigelaar RE, Hayday AC. The distinct contributions of murine T cell receptor (TCR)gammadelta+ and TCRalphabeta+ T cells to different stages of chemically induced skin cancer. J Exp Med 2003; 198:747-55; PMID:12953094; http://dx.doi.org/10.1084/jem.20021282
30. Yusuf N, Nasti TH, Katiyar SK, Jacobs MK, Seibert MD, Ginsburg AC, Timares L, Xu H, Elmets CA. Antagonistic roles of CD4+ and CD8+ T-cells in 7,12-dimethylbenz(a)anthracene cutaneous carcinogenesis. Cancer Res 2008; 68:3924-30; PMID:18483278; http://dx.doi.org/10.1158/0008-5472.CAN-07-3059
31. Ortiz ML, Kumar V, Martner A, Mony S, Donthireddy L, Condamine T, Seykora J, Knight SC, Malietzis G, Lee GH et al. Immature myeloid cells directly contribute to skin tumor development by recruiting IL-17-producing CD4+ T cells. J Exp Med 2015; 212:351-67; PMID:25667306; http://dx.doi.org/10.1084/jem.20140835

32. Wang L, Yi T, Zhang W, Pardoll DM, Yu H. IL-17 enhances tumor development in carcinogen-induced skin cancer. Cancer Res 2010; 70:10112-20; PMID:21159633; http://dx.doi.org/10.1158/0008-5472.CAN-10-0775
33. Nardinocchi L, Sonego G, Passarelli F, Avitabile S, Scarponi C, Failla CM, Simoni S, Albanesi C, Cavani A. Interleukin-17 and interleukin-22 promote tumor progression in human nonmelanoma skin cancer. Eur J Immunol 2015; 45:922-31; PMID:25487261; http://dx.doi.org/10.1002/eji.201445052
34. Nemunaitis J, Barve M, Orr D, Kuhn J, Magee M, Lamont J, Bedell C, Wallraven G, Pappen BO, Roth A et al. Summary of bi-shRNA/GM-CSF augmented autologous tumor cell immunotherapy (FANG) in advanced cancer of the liver. Oncology 2014; 87:21-9; PMID:24968881; http://dx.doi.org/10.1159/000360993
35. Ghisoli M, Barve M, Mennel R, Lenarsky C, Horvath S, Wallraven G, Pappen BO, Whiting S, Rao D, Senzer N et al. Three Year Follow up of GMCSF/bi-shRNA DNA Transfected Autologous Tumor Immunotherapy (Vigil) in Metastatic Advanced Ewing's Sarcoma. Mol Ther 2016; 24:1478-83; http://dx.doi.org/10.1038/mt.2016.86
36. Huang YH, Lin KH, Liao CH, Lai MW, Tseng YH, Yeh CT. Furin overexpression suppresses tumor growth and predicts a better postoperative disease-free survival in hepatocellular carcinoma. PLoS One 2012; 7:e40738; PMID:22808247; http://dx.doi.org/10.1371/journal.pone.0040738
37. Declercq J, Brouwers B, Pruniau VP, Stijnen P, Tuand K, Meulemans S, Prat A, Seidah NG, Khatib AM, Creemers JW. Liver-Specific Inactivation of the Proprotein Convertase FURIN Leads to Increased Hepatocellular Carcinoma Growth. Biomed Res Int 2015; 2015:148651; PMID:26167473; http://dx.doi.org/10.1155/2015/148651
38. Jakowlew SB. Transforming growth factor-β in cancer and metastasis. Cancer Metastasis Rev 2006; 25:435-57; PMID:16951986; http://dx.doi.org/10.1007/s10555-006-9006-2
39. Donkor MK, Sarkar A, Li MO. Tgf-beta1 produced by activated CD4 (+) T Cells antagonizes T Cell surveillance of tumor development. Oncoimmunology 2012; 1:162-71; PMID:22720237; http://dx.doi.org/10.4161/onci.1.2.18481
40. Cordova ZM, Grönholm A, Kytölä V, Taverniti V, Hämäläinen S, Aittomäki S, Niininen W, Junttila I, Ylipää A, Nykter M, Pesu M. Myeloid cell expressed proprotein convertase FURIN attenuates inflammation. Oncotarget. 2016 [Epub ahead of print] PubMed; PMID:27527873; http://dx.doi.org/10.18632/oncotarget.11106